

FOCUS REFLEX MODULATION OF ELECTRON GUNS*

Dr. Kurt Schlesinger
Consulting Engineer
Cathode Ray Tube Department
General Electric Company
Electronics Park
Syracuse, New York

*Part of the work reported here was done under Contract DA36-039 sc-78299
sponsored by the U. S. Army Signal Corps, Ft. Monmouth, N. J.

CAPTIONS

| <u>Figure No.</u> | <u>Caption</u> |
|-------------------|--|
| 1 | Hyperbolic Lens Field |
| 2 | Symmetrical Lens Modulator |
| 3 | Minimum Potential in a Focused Hyperbolic Lens |
| 4 | Focus Reflex Gun Assembly |
| 5 | Exploded View of Focus Reflex Gun |
| 6 | Characteristics of FRM Gun: one division= 50uA vertical, 2 volts horizontal. Pictures taken at aperture voltage of 150, 200, 250 and 300 volts respectively. |
| 7 | Current Distribution in Focus Reflex Gun |
| 8 | Overall Current Transmission for Various Ulterior Voltages |
| 9 | Television Test Pattern including Photographic Center Enlargement |
| 10 | Comparative Pulse Test, FRM vs. Standard Gun. Scope shows ulterior currents at 250uA per division. |

Summary. High resolution and low drive features have been successfully combined in a new type of electron gun for cathode ray tubes. The gun has a spot-defining aperture of .007" upon which emission from a large cathode area is concentrated by a retarding electron lens. This unit modulates the beam by electron reflection, while focusing it upon the aperture. ("Focus Reflex Modulation").

Immediately ahead of the aperture, a modulated virtual cathode is formed with an emission capability of over four amperes per cm^2 .

A 1000-microamperes beam with a six-degree divergence is controlled by a signal of 12 volts centered at ground potential. Highlight brightness of 250 foot lamberts was read at 17,500 volts, while more than 500 lines were resolved on a television test pattern.

I. Introduction

In recent years continued efforts have been made to achieve major improvements in the performance of cathode ray tubes. These efforts were stimulated, partly by the ever-present need for higher resolution, and partly by transistorization, which called for operation with low drive signals.

It was soon realized that major progress could hardly be expected from a mere extrapolation of conventional approaches. Instead, several novel and interesting gun designs have been developed, all capable of operation with signals below the ten-volt level. ^{1, 2, 3, 4} To satisfy the need for better resolution, some of these guns used spot-defining apertures whose basic advantage over conventional crossover-imaging systems was early recognized by R. R. Law many years ago. ⁵

After reviewing the present state of the art, the Signal Corps formulated several performance features which were considered desirable in a modern CRT gun of advanced design. These specifications included a defining aperture of small dimensions (.005"), strong beam currents (1000uA), and low drive

signals (below ten volts). In addition, an upper limit of six degrees was imposed for beam divergence in order to permit the use of conventional deflection components.

II. Approach to the Problem

A one-milliamperere beam passing through a defining aperture of seven mils presents there a local current density of four amp/cm². This is one order of magnitude above conventional figures for the loading of an oxide cathode.

Accordingly, it was decided to start with a large area Pierce cathode (diameter 30 mils, emission density 0.4 A/cm²), to collimate its emission into parallel flow, and then to focus it upon the aperture with considerable demagnification. This move was successfully executed by employing as a condenser lens, a symmetrical hyperbolic lens with low aberrations.⁶ However, this solved only part of the problem. The problem called for modulation to be done ahead of the aperture with restriction to devices with circular symmetry. This left practically no alternative but to use an electron mirror as the control element. Its use depended entirely on the feasibility of redesigning the condenser lens for focusing by deceleration. This would result in the formation of a virtual cathode at focus. If a signal was present in the process, this virtual cathode would be modulated. Our work has shown that this is practical. "Focus Reflex Modulation" (FRM) is a method of controlling beam intensity by a focused electron reflector.

III. Hyperbolic Electron Lens

Figure 1 presents some fundamentals about hyperbolic lenses. We first formulate the condition for a "proportional" radial force component:

$$\frac{1}{\epsilon} \cdot F_r = -c \cdot r = \frac{\partial U}{\partial r} \quad (1)*$$

*Note that these forces are independent of axial position z. That makes the hyperbolic lens essentially mono-energetic.

This is entered into the Laplacian equation for the space potential, $U(r, z)$. The solution is found to be:

$$U = V_m + c \left[(z - z_m)^2 - \frac{1}{2} r^2 \right] \quad (2)$$

Rewritten in the form shown in Figure 1a, the equipotentials are found to be hyperboloids of revolution about the z axis. All of these share, as a common asymptote, a double cone with the apex angle of $109^\circ 24'$. Within this lens volume, it is found that the second derivative d^2V/dz^2 of the axis potential, V , is a constant, namely $2c$. The quantity c is the refractive power of the lens, and its sign indicates, respectively, positive or negative lens action.

Figure 1c is a cut through a hyperbolic lens by an axial plane. The electron beam enters from the left through a hole in the first anode at voltage V_0 , and is then subjected to radial restoring forces before leaving a small aperture in the second anode at voltage V_ℓ .

In any practical application of a hyperbolic lens several important parameters remain to be determined. These include:

- 1) the position, z_m , of the focusing electrode and its bias, W_g ,
- 2) the total length, ℓ , of the system, and
- 3) the output anode voltage, V_ℓ , defined by its acceleration ratio

$$P = V_\ell / V_0 \text{ over the input voltage, } V_0.$$

Complete and unique information about these variables is forthcoming from a study of the trajectories inside the lens, as will be seen below in Section V.

IV. Modulation in a Symmetrical Lens

Figure 2 shows an early test which helped to point out the basic design problem for a lens modulator. A symmetrical ($z_m = \ell/2$), non-accelerating lens

was used (Figure 2a), to focus a parallel beam through A_1 , upon a small aperture in A_2 , both anodes being at the same voltage. The center electrode, G, was connected to the signal. Beam current, I_b , through the aperture was measured at a collector plate, P, behind the anode A_2 . Total current, I_t , through the control gate, G, was measured in the A_2 return. This current included I_b as well as the current intercepted at the aperture.

Figure 2b shows the control function of the gate which included cutoff and saturation of I_t at negative voltages, e_c and e_s , respectively. This range of lens operation is henceforth referred to as the Reflector Mode or RM.

Figure 2c shows the beam current, I_b , as collected behind the aperture. This curve repeats the RM mode in the range around cutoff, i.e. between e_c and e_s . However, Figure 2c also shows a peak of output, three times stronger than the open gate current, and occurring at a much more positive gate voltage, e_f . This peak is due to beam focusing upon the aperture.

The test made it clear that in a three-element lens, there is no inherent coincidence between voltages required for focusing and control. In its absence, maximum power output is not available and the shape of the characteristic becomes unusable. Hence, if voltage coincidence were realizable at all, it must be brought about by electron-optical design. Specifically, in a hyperbolic lens of the non-accelerating type, the focus voltage, e_f , is much too positive to become contingent to the open-gate voltage, e_s . It will be shown below that Focus Reflex Modulation requires the use of a half-section, non-symmetrical type of hyperbolic lens, and that the focusing field must be wholly of the retarding type.

V. Electron Trajectories in a Modulating Lens

In a field as given by equation 2, the equations of motion take the form:

$$\begin{aligned}\ddot{r} &= \eta \frac{\partial \mathcal{U}}{\partial r} = -c \eta r \\ \ddot{z} &= \eta \frac{\partial \mathcal{U}}{\partial z} = 2 \eta c (z - z_m)\end{aligned}\quad (3)$$

and the trajectories are expressed by:

$$r = r_0 \cos \omega t + \frac{\dot{r}_0}{\omega} \sin \omega t \quad (4)$$

$$z = z_m (1 - \cosh \sqrt{2} \omega t) + \sqrt{\frac{V_0}{c}} \sinh \sqrt{2} \omega t \quad (5)$$

where $\omega = \sqrt{\eta c}$ is the "frequency" of the lens and $\eta = e/m$. If the beam is to reach the output at $z = l$ with a velocity of V_e (volt), we get:

$$\sqrt{\frac{V_e}{c}} = -z_m \sinh \sqrt{2} \varphi + \sqrt{\frac{V_0}{c}} \cosh \sqrt{2} \varphi \quad (6)$$

$$l = z_m (1 - \cosh \sqrt{2} \varphi) + \sqrt{\frac{V_0}{c}} \sinh \sqrt{2} \varphi \quad (7)$$

Here, $\varphi = \omega T$ is the flight-phase, and T is the transit time through the lens. z_m is the position of the saddle point of potential V_m and also the position of the control electrode, G. (See Figure 5). Solving equations 6 and 7 for φ and z_m yields:

$$\tanh(0.707 \varphi) = \frac{l \sqrt{c}}{\sqrt{V_0} + \sqrt{V_e}} \quad (8)$$

$$\frac{z_m}{\frac{1}{2} l} = 1 + \frac{V_0}{l c^2} (1 - P) \quad (9)$$

These equations are, thus far, not limited to any specific mode of operation of the hyperbolic lens.

We now introduce the condition, that the lens should become "self-focusing", i.e. that the focal point formed from a collimated beam should fall into the aperture. Equation 4 tells that all parallel rays ($\dot{r}_0 = 0$) will reach the axis ($r = 0$) after a flight phase of 90-degrees ($\varphi = \frac{\pi}{2}$). The lens power of required for self-focus, then follows from equation (8) for $\varphi = \frac{\pi}{2}$:

$$c_f = 0.64 \frac{V_0}{\ell^2} (1 + \sqrt{P})^2 \quad (10)$$

If this value is entered into equation 9 and 2, we obtain the desired information about the saddle potential, V_m , and its position, z_m , within a self-focusing, hyperbolic lens:

$$\frac{z_m}{\ell} = \frac{1}{2} + 0.78 \frac{1 - \sqrt{P}}{1 + \sqrt{P}} \quad (11)$$

$$\frac{V_m}{V_0} = 1 - 1.05 [1 - 0.22 \sqrt{P}]^2 \quad (12)$$

These results are plotted graphically in Figure 3 as functions of the parameter $P = V_\ell / V_0$, i.e. the voltage ratio across the lens.

The outstanding lesson from Figure 3 is that low values of the saddle potential can be realized only by placing the gate electrode close to the exit of the lens. In the ultimate, the gate coincides with the asymptotic cone and the lens is completely non-symmetrical.

The table shown in Figure 3 points out that the saddle potential, V_m , for focus can run as high as $0.36 \cdot V_0$, or +90 volts, if the lens is symmetrical, ($z_m = 1/2 \ell$). On the other hand, V_m drops as low as =12.5 volts for a non-

symmetrical lens whose gate electrode has been pushed back close to the final anode, $z_m = \ell$. --In the first case, the potential, V_m , for focus is too far positive to blend into the reflector mode, and a "fractured" characteristic results, (see Figure 2).--In the second case, the low gate potential e_f , required for self-focus is about the same as the "open gate" voltage, e_s , thus providing the best electron optical transmission when the largest beam current passes the gate.

VI. Final Form of Focus Reflex Gun

Figure 4 shows the gun assembly for Focus Reflex Modulation. Its design is closely related to the theory just described. The gun uses a Pierce cathode, K, followed by a grounded collimator, C, and a plane-convex anode, A. This emission system is dimensioned such as to deliver a parallel unmodulated beam of 1800uA at a specified anode voltage (500 volts), and with normal cathode loading ($0.4A\text{ cm}^{-2}$).

A decelerating, hyperbolic lens field is formed between the convex surface of A and the 109-degree, conical profile of the gate electrode, G. The total flight path from anode to apex measures one-half of the radius of anode curvature. If the gate is connected to a 12-volt signal source, centered around zero bias, a modulated virtual cathode is formed at the apex of the cone, G. This virtual cathode has an approximate diameter of .005" and has a potential peak emission density of ten amp/cm⁻².*

A low voltage anode, M, (+250V) supporting the spot-defining aperture (.007") is brought up very close (.008") to this virtual cathode. The signal voltage at the gate determines the fraction of current to be forwarded through the aperture in M, while the remainder is reflected back to the preceding anode, A. The forward current past the aperture diverges heavily (14 degrees), but it is reconverged to below seven degrees by a short

* These data are obtained by considering the observed beam output through the aperture as coming from an equivalent spherical diode.

accelerating field which exists between the 109-degree profile in the meniscus anode and the end plate of the main lens barrel, B.

Figure 5 shows a photograph of the completed FRM gun assembly, including an exploded view of some of the parts.

VII. Performance Data

Figure 6 shows the current past the aperture as a function of gate voltage taken for various values of d-c voltage on the aperture. The characteristic shows currents of 900 to 1000 μ A fully controlled by signals of 11 to 12 volts with 250 and 300 volts at the aperture, respectively. A log-log plot of the same curve is straight from 50 μ A to 1000 μ A. This implies that Focus Reflex Modulation follows a power law with a gamma of 2.6 over most of its useful range. The transconductance increases with current to a maximum of about 180 μ A/volt; the average g_m is about one-half of this value.

As the meniscus voltage is decreased, a discontinuity of current seems to develop which is quite evident in the curve for $M = 150$ volts. We believe this to be due to a depression of the minimum potential by space charge. In fact, this break is predicted correctly by the well-known formula for limiting current through a drift tube⁷:

$$I_{max} = 1230 \cdot V_{KV}^{3/2} \cdot \left(\frac{d}{l}\right)^2 \quad (13)$$

when entering the dimensions of the grid throat and assuming a beam velocity of ten volts. Fortunately, this condition is safely avoided in practice by using adequate positive voltages at the aperture.

Figure 7 shows the current distribution in the FRM gun. The current I_2 , reflected back to anode, A_1 , keeps a relation of complementary symmetry with respect to forward current, I_b . Interception, I_m , at the aperture is less than 15 percent of cathode current, and gate-current drain is negligible. The gate capacitance is 7mmf.

Figure 8 shows the screen current in percent of cathode emission. This is the overall transmission efficiency of the gun. It reads 60 percent at 15KV and 73 percent at 20KV. This increase is due to the fact that the reconverging field at the aperture is more efficient at higher values of voltage step-up there. The sample gun used a conventional bi-potential lens with stops for a beam spread of seven degrees.

Figure 9a shows a standard television resolution test. Figure 9b is a separate photograph of the center section of Figure 9a, taken with an enlarged scale to facilitate photographic reproduction. These pictures measured 250 foot lamberts in the highlights with 17,500 volts screen voltage and with 11 volts video drive. In the same test position a conventional picture tube gave 90 foot lamberts with over 50 volts drive.

An electron gun with a defining aperture is expected to show better resolution and less spot swell at high currents than a conventional gun with cathode crossover. To verify this point, a comparative test was done with pulsed operation of a 14-inch picture tube of conventional design and of a 14-inch tube using the FRM gun. Figure 10 shows a slow circular scan (60 cps, 2" circle) displaying twelve 40-microsecond pulses of varying amplitude. Figure 10c shows the screen current pulses in the return to Dag. These pulses were adjusted to read equal peak value (700uA) for both tubes. Grid drive requirements were 60 volts and 11 volts, respectively.

Figure 10a shows the performance of a conventional television picture tube. Measured over a current range from 50 to 650 microamperes, the apparent spot size increased from 30 mils to 120 mils.--In the FRM tube, the corresponding readings were 40 mils and 60 mils (Figure 10b). This test illustrates the benefits from the use of a defining aperture. Spot swell with current is reduced to less than one-half and there is a corresponding gain in resolution at very high light levels.

VIII. Acknowledgement

The author is indebted to members of the cathode Ray Tube Department for their help, interest and encouragement. This includes Messrs. C. Dichter, Manager of the Industrial and Military Operation, P. E. Sullivan, Manager of Product Engineering, and E. F. Schilling, Manager of Electron Optics Design Sub-section. Thanks are due to P. Coppola and to his assistant for preparation of special cathodes, and, last but not least, to Messrs. P. Lemire and R. Wagner who directly cooperated with the author on the project.

Literature References

1. E. Atti: "High Transconductance Wide-band Television Gun," 1958 IRE National Convention Record, Part III - Electron Devices, P. 3.
2. K. Schlesinger: "A New Electron Gun for Low Drive Signals", IRE Transactions on Electron Devices, Vol. ED-6, No. 4, October 1959, P. 377.
3. J. W. Schwartz: "The Annular Geometry Electron Gun", 1958 IRE National Convention Record, Part III - Electron Devices, P. 13.
4. P. Gleichauf: "Space-Charge Grid High-Transconductance Guns", Proceeding IRE, Vol. 46, No. 8, August 1958, P. 1542. And, "Crossed Cylindrical Lens High-Transconductance Guns", Proceedings IRE, Vol. 47, No. 1, January 1959, P. 95.
5. R. R. Law: "High Current Electron Gun for Projection Kinescopes", Proceedings IRE, Vol. 25, No. 8, August 1947, P. 954, 976.
6. R. Rudenberg: "Electron Lenses of Hyperbolic Field Structure", Journal Franklin Institute, October and November, 1948, P. 311-339 and 337-408.
7. K. Spangenberg: Electron Tubes, first edition P. 447, McGraw-Hill Co., 1948.

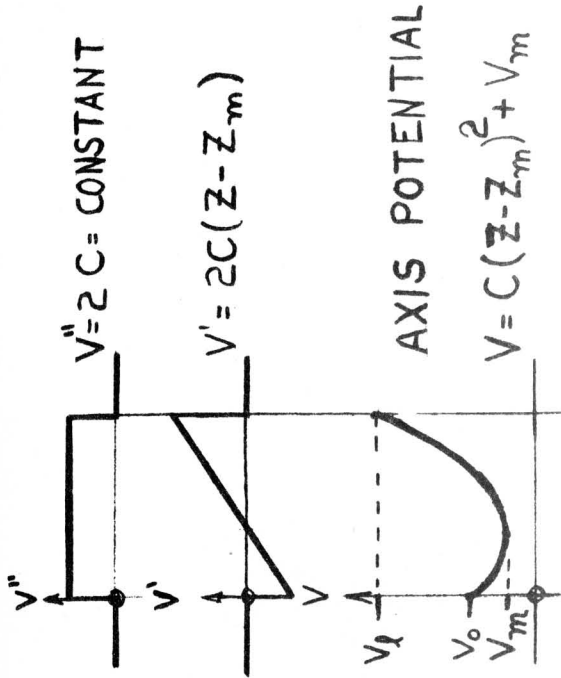
$$\frac{1}{\epsilon} \cdot F_R = -C \cdot r = \frac{\partial u}{\partial r}$$

$$\frac{\partial^2 u}{\partial r^2} + \frac{1}{r} \frac{\partial u}{\partial r} + \frac{\partial^2 u}{\partial z^2} = 0$$

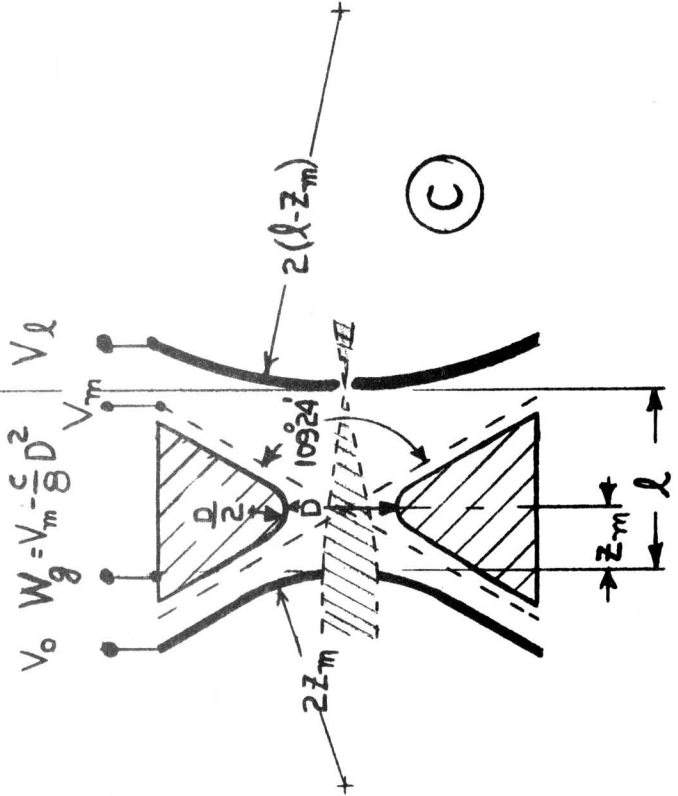
$$\frac{\partial^2 u}{\partial z^2} = \frac{d^2 V}{dz^2} = 2C = \text{CONSTANT}$$

SPACE POTENTIAL $u(r, z)$

$$\frac{(z - z_m)^2}{\frac{u - V_m}{C}} - \frac{r^2}{2 \frac{u - V_m}{C}} = 1$$



(B)



(A)

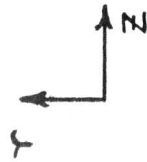


Figure 1

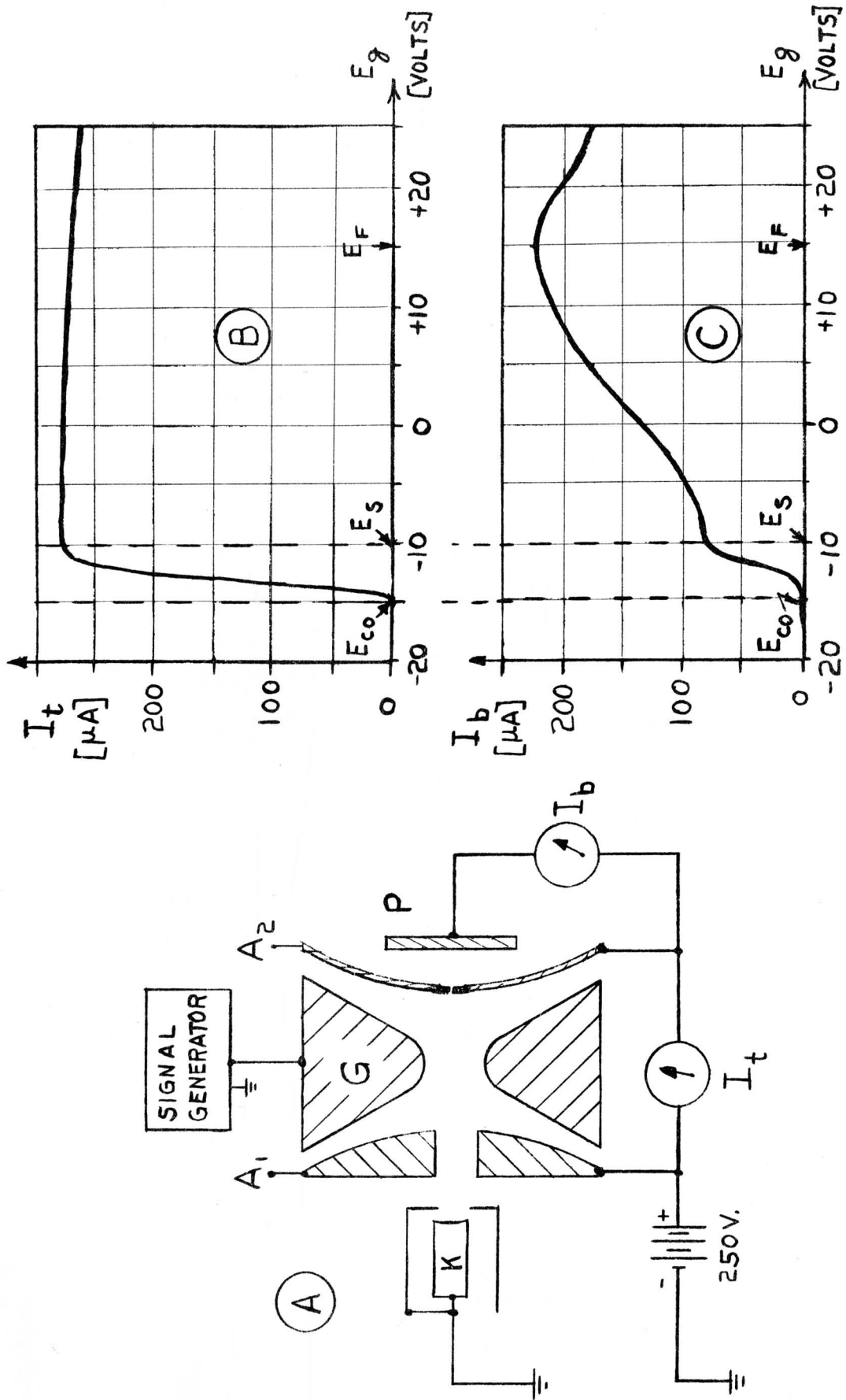


Figure 2

$$\frac{z^m}{l} = 0.5 + 0.78 \frac{1 - \sqrt{P}}{1 + \sqrt{P}}$$

$$\frac{V_m}{V_0} = 1 - 1.05 [1 - 0.22\sqrt{P}]^2$$

| $P = \frac{V_l}{V_0}$ | $\frac{z^m}{l}$ | $\frac{V_{min}}{V_0}$ |
|-----------------------|-----------------|-----------------------|
| 1.0 | 0.5 | 0.36 |
| .048 | 1.0 | 0.05 |
| .013 | 1.28 | 0 |

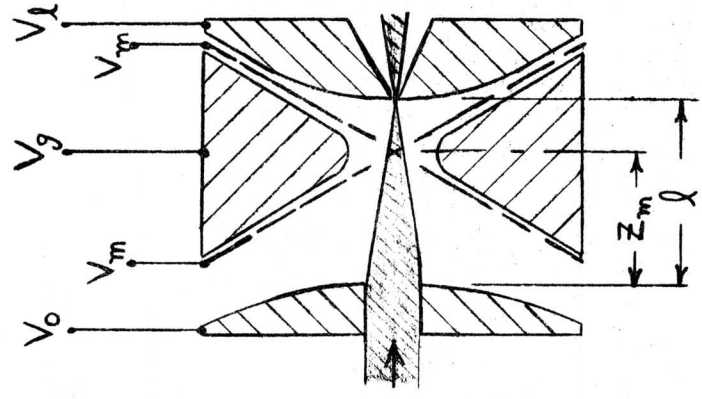
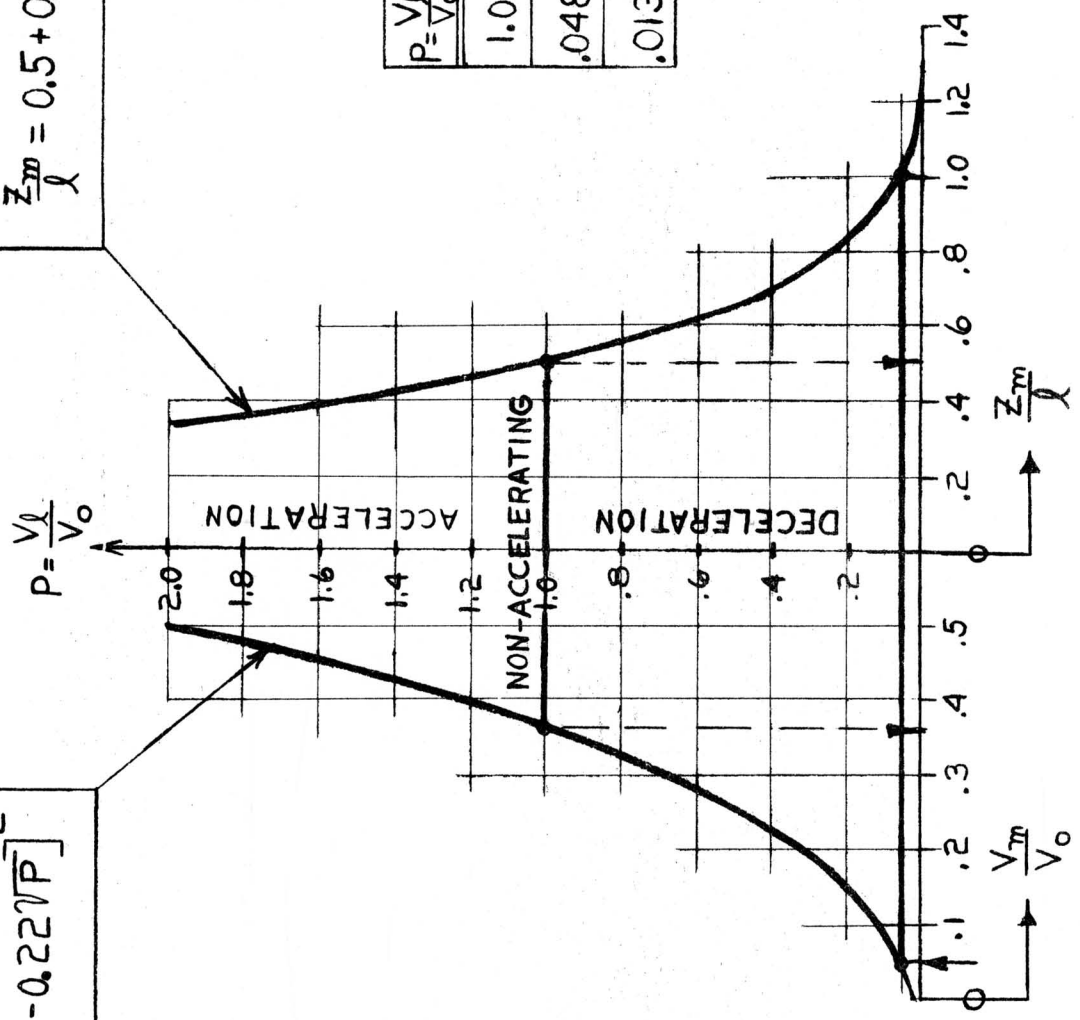


Figure 3

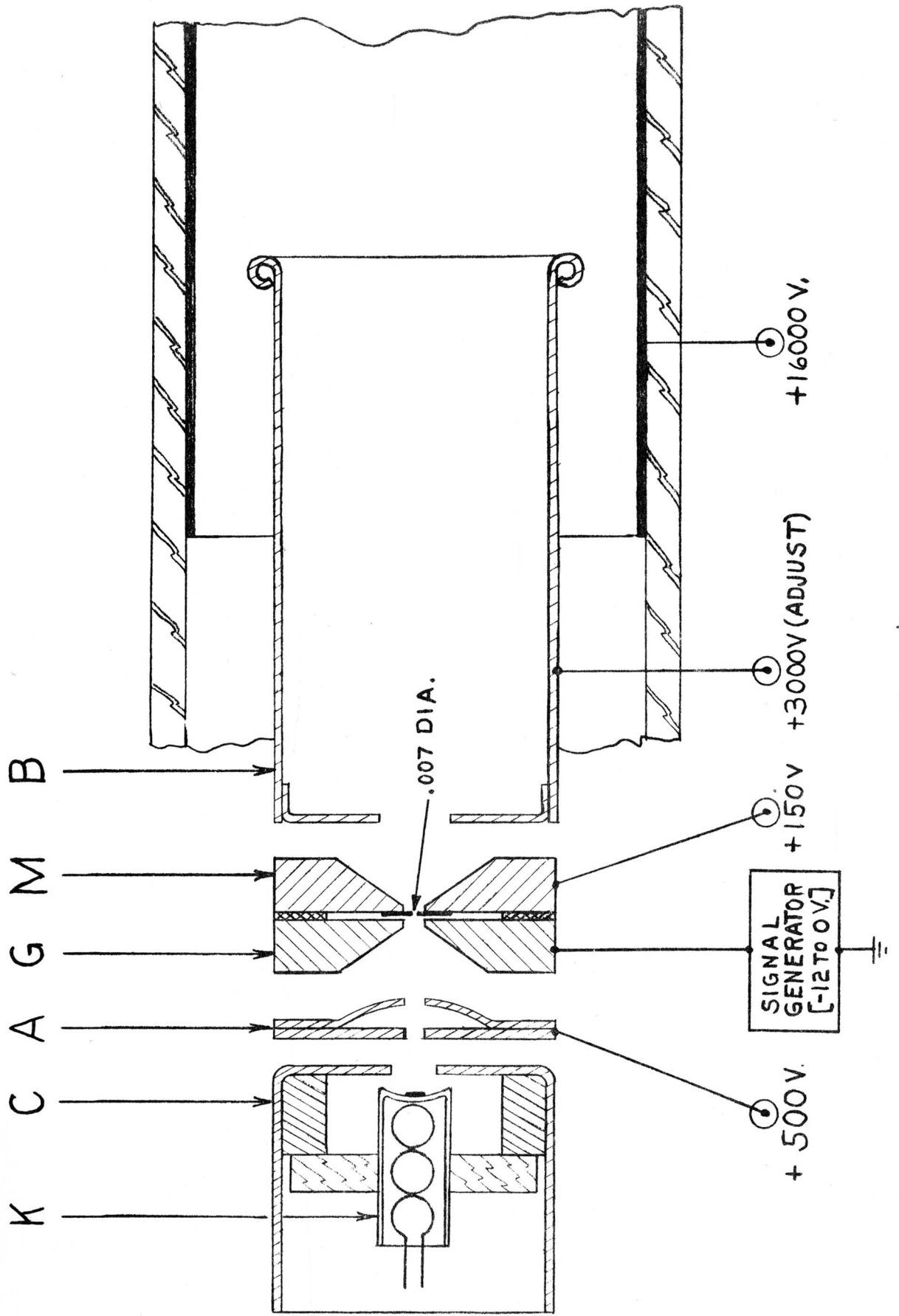


Figure 4

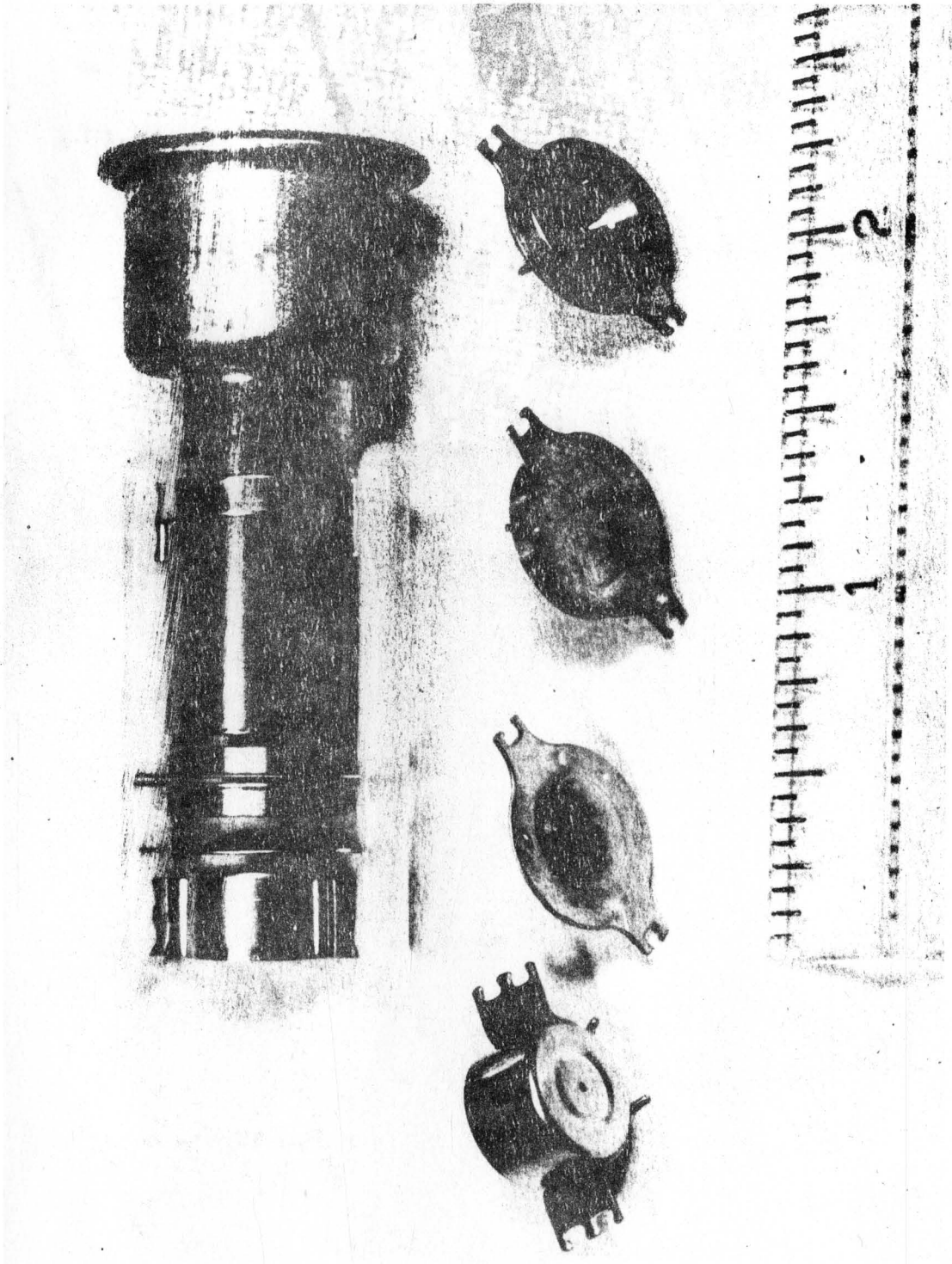


Figure 5

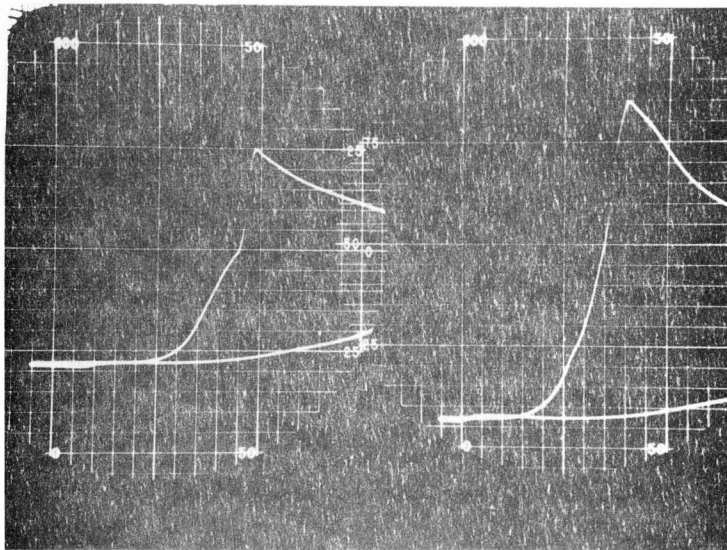
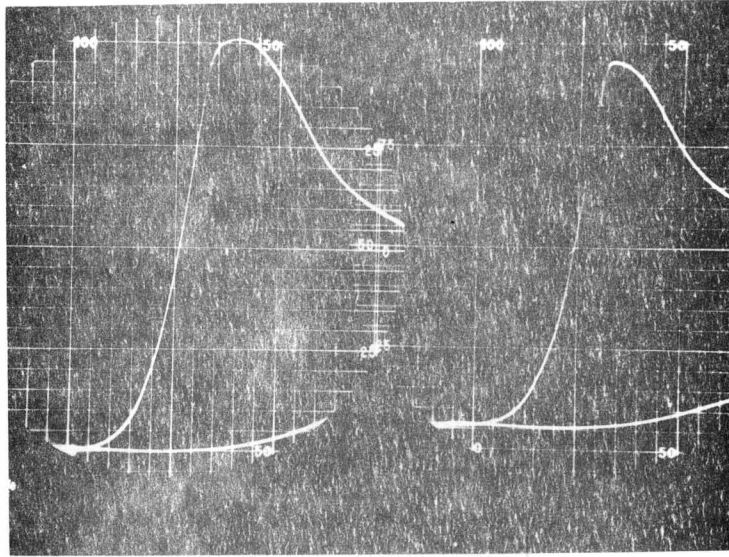


Figure 6

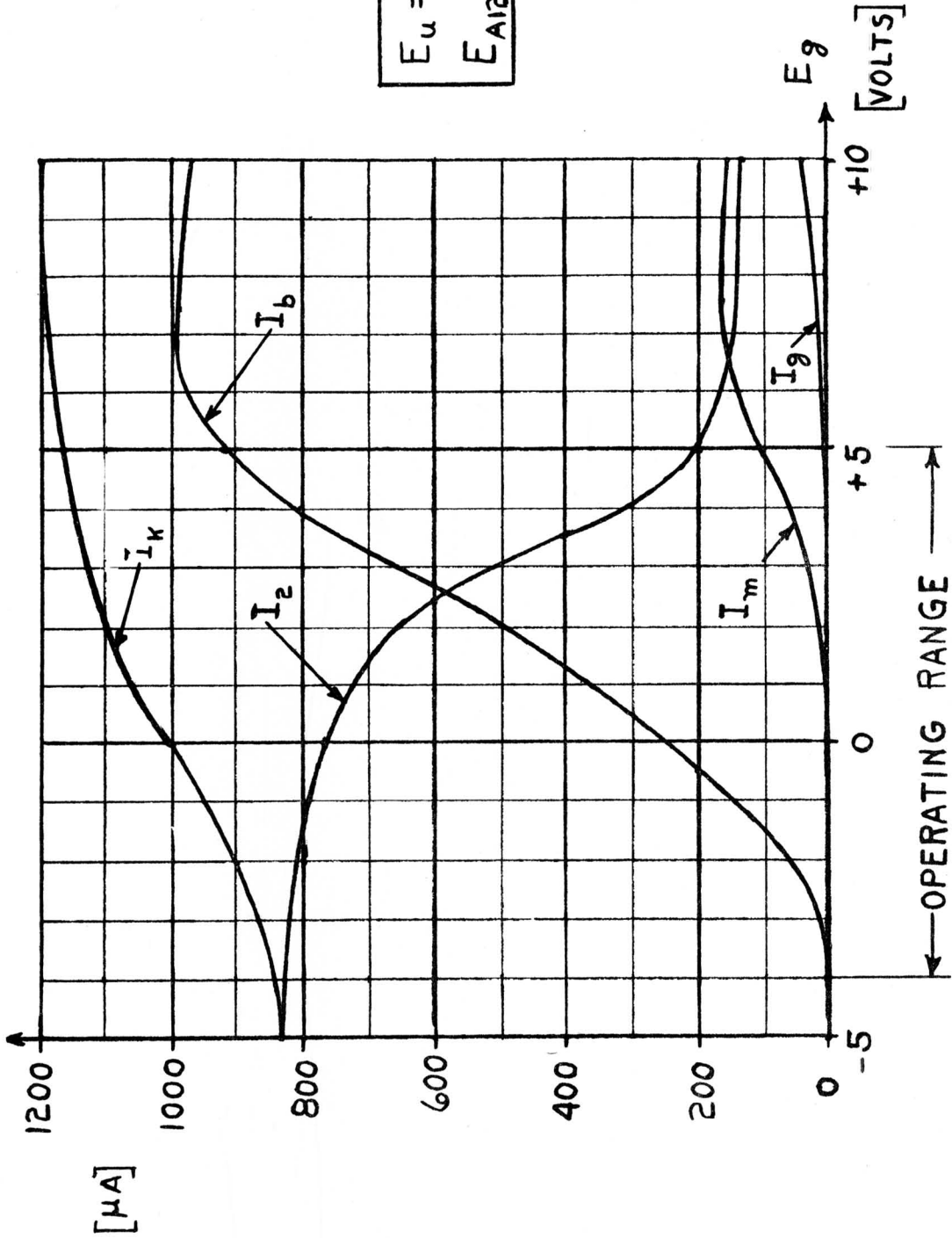


Figure 7

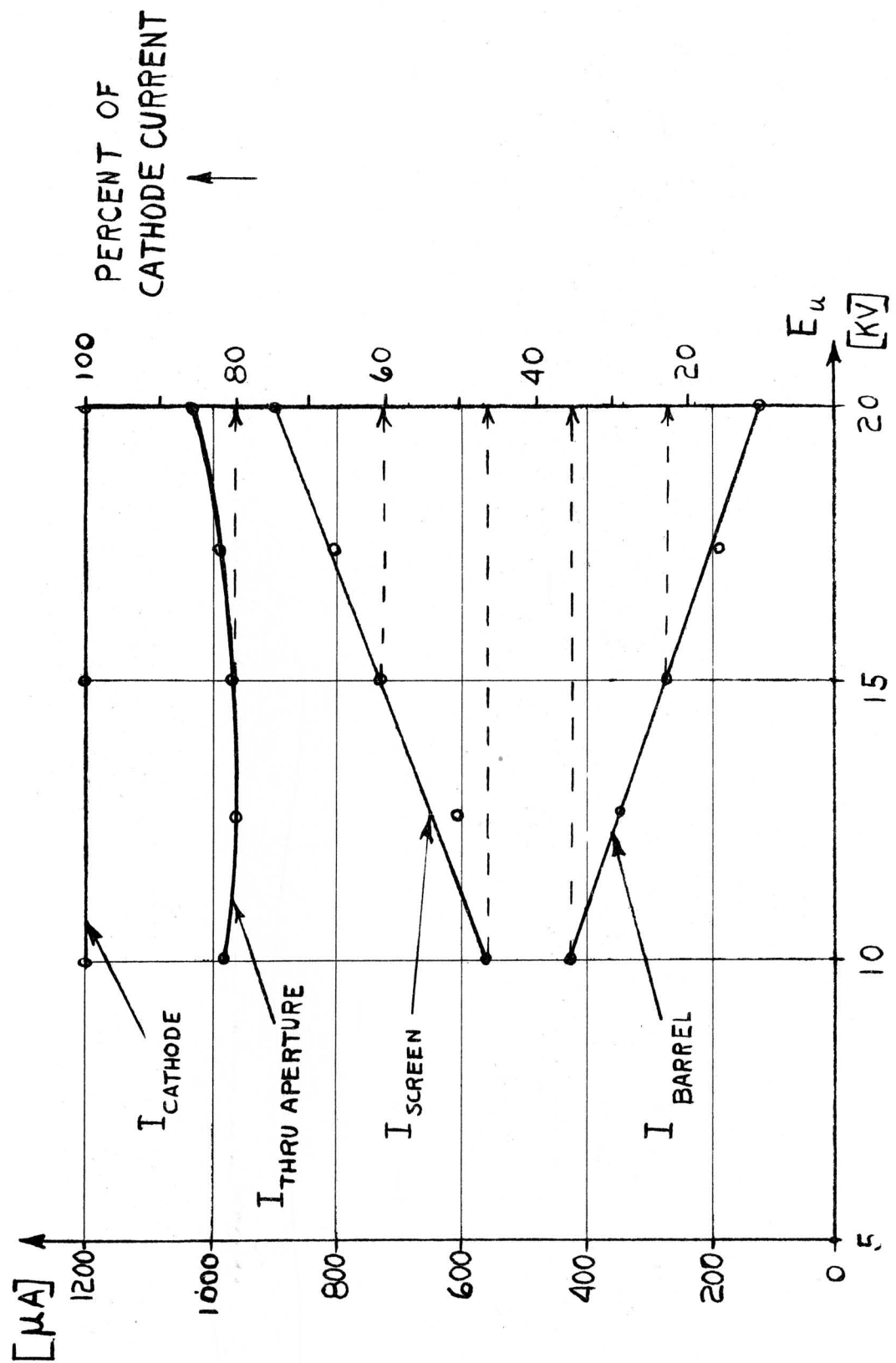


Figure 8

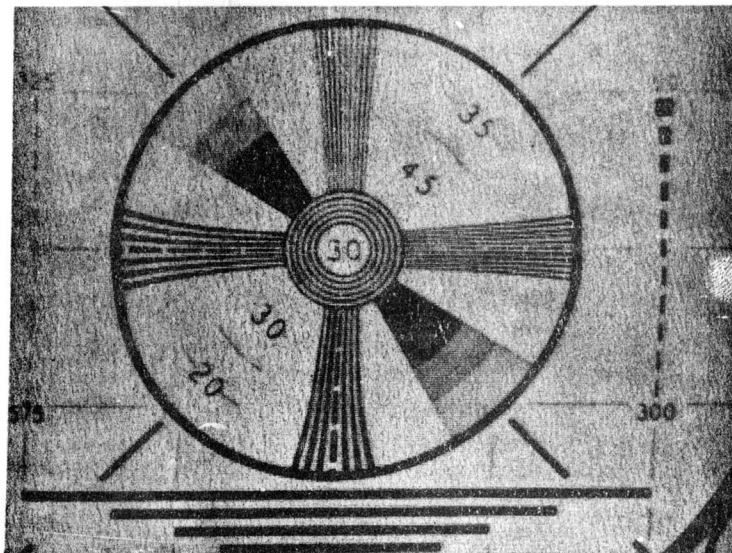
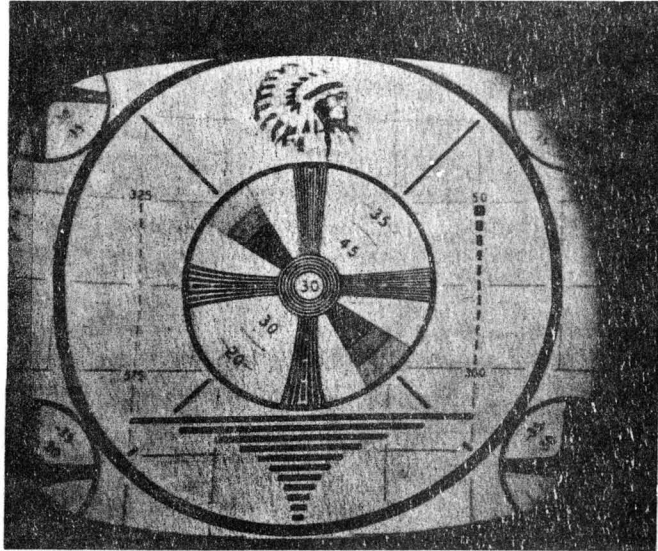


Figure 9

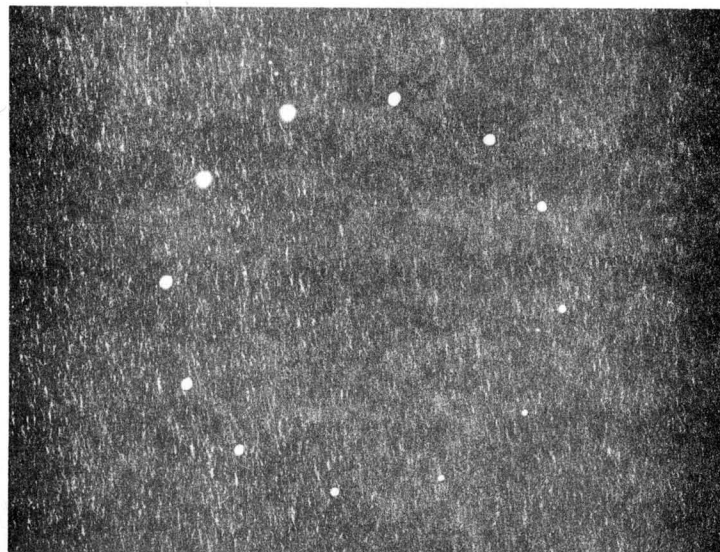
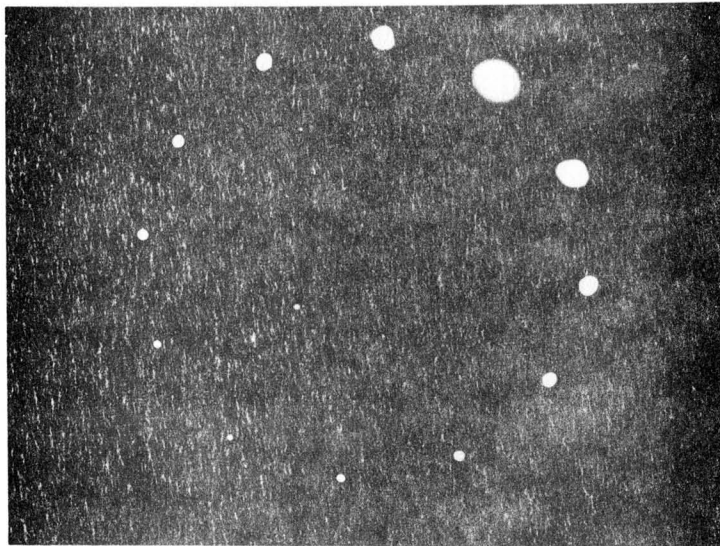
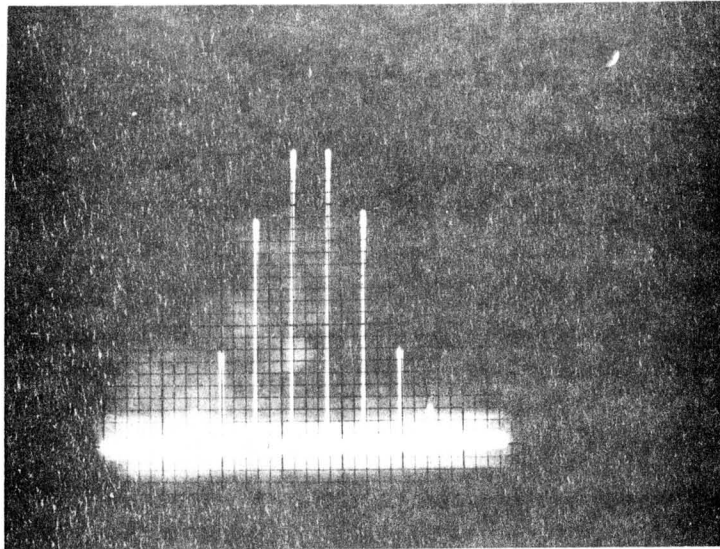


Figure 10